DOI: 10.1002/ejic.200700598

# Electrochemical Synthesis of Mono- and Disubstituted Diiron Dithiolate Complexes as Models for the Active Site of Iron-Only Hydrogenases

**Didier Morvan,[a] Jean-François Capon,[a] Frederic Gloaguen,*[a] Philippe Schollhammer,[a] and Jean Talarmin[a]**

**Keywords:** Biomimetic catalysis / Iron-only hydrogenases / Diiron dithiolate / CO substitution / Electrochemistry / Proton reduction

$[Fe_2(S_2C_3H_6)(CO)_5\{P(OMe)_3\}]$ (**2**) and $[Fe_2(S_2C_3H_6)(CO)_4\{P(OMe)_3\}_2]$ (**3**) were selectively prepared by the electrochemical reduction of $[Fe_2(S_2C_3H_6)(CO)_6]$ (**1**) in the presence of trimethyl phosphite ligand. Electrochemical data indicate a CO-displacement reaction catalyzed by electron transfer. Complexes **2** and **3** were characterized by X-ray crystallography, which shows that in the solid state, the trimethyl phosphite ligands lie in the apical configuration. NMR suggests that multiple isomers exist in solution. Both **2** and **3** exhibit a primary reduction step that involves two electrons. No stable hydride derivatives could be isolated by the reaction of **2** or **3** with strong acid. However, for both **2** and **3**, proton reduction catalysis was detected at a potential less negative than that of the reduction of the diiron complex working as catalyst. The proposed mechanism involves a protonation of the diiron complex in the vicinity of the electrode, which is triggered by the more facile reduction of the protonated form (CE mechanism). The protonation and reduction steps are followed by a bimolecular reaction that regenerates the starting complex.


## Introduction

Hydrogenases are nickel- and iron-based enzymes that control the hydrogen production and uptake in a wide variety of microorganisms. These biomolecules have long interested biologists and chemists, as they might hold the key to a competitive hydrogen economy.[1] Recently, the active site of the iron-only hydrogenases was structurally characterized and shown to contain a dithiolate-bridged diiron moiety with carbonyl and cyanido ligands.[2] This has opened the way for the synthesis of organometallic models that could eventually work as cheap and efficient proton reduction catalysts.[3–11] The First structural models were readily accessed by the substitution of two CO ligands with two $CN^-$ ligands in $[Fe_2(S_2C_3H_6)(CO)_6]$ (**1**).[12–14] Several structural aspects of the iron-only hydrogenase active site have been modeled by diiron complexes bearing azadithiolate and related bridges,[15–18] a 2Fe3S core,[19,20] or chelating ligands.[21–26] Mimicking the catalytic activity of the hydrogenases turns out to be far more challenging. For the all-carbonyl complex **1**, the catalysis of proton reduction in acidified acetonitrile solution requires potentials more negative than –1.6 V[27,28] (all potentials in this paper are referenced to that of the reversible oxidation of ferrocene, $E_{1/2}^{ox}$ = 0.4 V vs. NHE). The substitution of one or two CO ligands by good donor ligands such as cyanido, phosphane, and/or *N*-heterocyclic carbene (NHC) yielded better functional models.[21,29–33] Good donor ligands increase the basicity of the iron–iron bond, and thus render it susceptible to protonation by relatively strong acids ($pK_a < 10$).[34,35] On protonation, the reduction potential of the complex is positively shifted by about 1 V, and catalytic hydrogen evolution can be detected at potentials around –1.4 V.[29,30] This obviously suggests that advances in designing an efficient proton reduction catalyst will follow from a greater balance between the basicity and the reduction potential of the diiron center. There are several examples of $[Fe_2(SR)_2(CO)_{6-x}L_x]$ ($x$ = 1, 2) complexes with ligands L that have a relatively modest donor ability such as phosphite or isocyanide.[36–40] However, the electrochemistry of these compounds and their reactivity toward protons have so far received little attention. In addition, they were generally prepared in rather low yields by thermal activation to give a mixture of mono-, di-, and trisubstituted derivatives. On the other hand, it was shown that electron transfer (reduction or oxidation) could also lead to substituted diiron dithiolates.[38,41,42] For example, the formation of $[Fe_2(S_2C_2H_4)(CO)_5\{P(OMe)_3\}]$ by an electron-transfer-catalyzed chain reaction was detected upon the electrochemical reduction of the all-CO parent compound in the presence of $P(OMe)_3$.[41] A similar approach allowed us to

[a] UMR CNRS 6521: Chimie, Electrochimie Moléculaires et Chimique Analytique, Université de Bretagne Occidentale, CS 93837, 29238 Brest, France
Fax: +33-298-017001
E-mail: fgloague@univ-brest.fr
Supporting information for this article is available on the WWW under http://www.eurjic.org or from the author.

  

selectively prepare $[Fe_2(S_2C_6H_4)(CO)_5\{P(OMe)_3\}]$ in good yield.[43]

We now describe the selective synthesis of $[Fe_2(S_2C_3H_6)(CO)_5\{P(OMe)_3\}]$ (**2**) and $[Fe_2(S_2C_3H_6)(CO)_4\{P(OMe)_3\}_2]$ (**3**) by bulk electrolysis of the all-CO parent compound **1** in the presence of $P(OMe)_3$. The purpose of this preliminary study was to determine whether electrochemical methods could be used as a general route for the selective preparation of mono- and disubstituted diiron dithiolates. The crystallographic and spectroscopic characterization and the electrochemical properties of complexes **2** and **3** are also reported.

## Results and Discussion

### Preparation and Characterization of Complexes 2 and 3

IR spectra recorded over a period of several hours showed that a $CH_3CN$ solution of the all-CO compound **1** was not reactive toward the addition of 1.1 molar equiv. of $P(OMe)_3$ at room temperature. However, electrolysis of this solution at a potential slightly more negative than the reduction potential of **1** readily gave the monosubstituted derivative **2**. The disubstituted complex **3** was similarly obtained by bulk electrolysis of a solution of **1** with 2.1 molar equiv. of $P(OMe)_3$ at a potential slightly more negative than the reduction potential of **2**. In each case, IR spectra indicated total consumption of **1** in 45–60 min. The charge passed in the course of electrolysis was about 0.7 F per mol of **1**, which indicates that CO-displacement reactions catalyzed by electron transfer occur (see Supporting Information).[41,43]

Compounds **2** and **3** were characterized by IR and NMR spectroscopy, elemental analysis, mass spectrometry, and X-ray crystallography. The shift in the $\nu_{CO}$ bands is considered a useful indicator of the variation in electron density in diiron models of the hydrogenase active site. The average values for the IR bands in the carbonyl stretching region are lowered by 47 and 79 $cm^{-1}$ for the monosubstituted compound **2** ($\tilde{\nu}_{CO}$: 2048, 1991, 1976, 1938 $cm^{-1}$) and the disubstituted compound **3** ($\tilde{\nu}_{CO}$ = 2004, 1966, 1937, 1917 $cm^{-1}$), respectively, relative to those in the all-CO compound **1** ($\tilde{\nu}_{CO}$: 2073, 2033, 1999 $cm^{-1}$). The redshifted values for **2** and **3** indicate that the electron-donating ability of $P(OMe)_3$ is comparable to that of $PPh_3$ and slightly better than that of $P(OEt)_3$ and *t*BuNC.[39,40] The difference in wavenumber between the highest and lowest band ($\Delta\tilde{\nu}_{CO}$ = 87 $cm^{-1}$) in **3** is smaller than that in the monosubstituted complex **2** ($\Delta\tilde{\nu}_{CO}$ = 110 $cm^{-1}$), which indicates that **3** is a symmetric diphosphite derivative.[25]

Evidence for monosubstitution in **2** was provided by $^{13}C$ NMR spectroscopy. The spectrum of **2** displays two carbonyl resonances: a doublet at $\delta$ = 211.9 ppm assigned to the two carbonyl ligands of the $Fe(CO)_2[P(OMe)_3]$ moiety and a singlet at $\delta$ = 209.6 ppm assigned to the three carbonyl ligands of the $Fe(CO)_3$ moiety. The $^{13}C$ NMR spectrum of the disubstituted complex **3** shows only one doublet at $\delta$ = 213.5 ppm for the carbonyl ligands.

The dynamic properties of complexes **2** and **3** were investigated by variable temperature $^{31}P$ NMR spectroscopy. At room temperature, the NMR spectrum of complex **2** displays one signal at $\delta$ = 177.0 ppm, which splits at 183 K into four sharp resonances (186.4, 184.4, 178.0, and 177.1 ppm, Figure 1a). This indicates that the dynamic site exchange

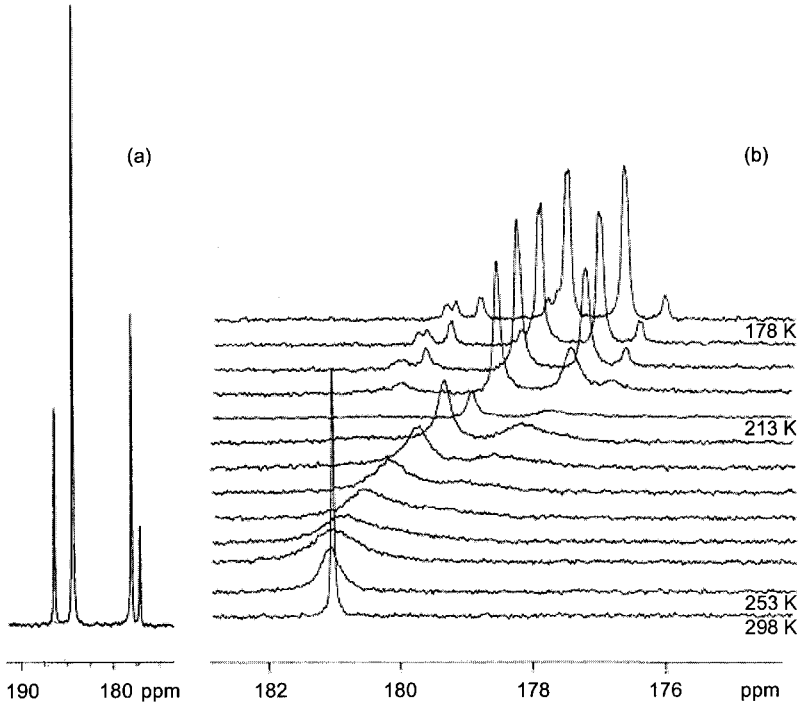


Figure 1. $^{31}P$ NMR spectra of (a) compound **2** at 183 K and (b) compound **3** at variable temperatures from 298 K to 178 K.

  

processes at low temperature are sufficiently slow on the NMR timescale to allow the detection of the four isomers expected for a monosubstituted derivative (Scheme 1). The fluxional processes that occur in solution are a basal/apical rotation of the phosphite and carbonyl ligands along with a flipping of the methylene group of the propanedithiolate ligand.[44,45]

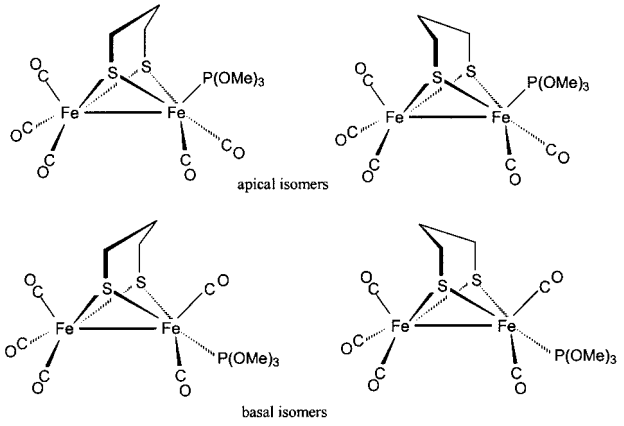


Scheme 1.

At room temperature, the $^{31}P$ NMR spectrum of **3** displays one signal at $\delta$ = 180.4 ppm (Figure 1b). The $^{31}P$ NMR pattern at 183 K suggests the presence of the four expected isomers, relative to the position of the phosphite ligands (Scheme 2). The major isomer (75%) displays four poorly resolved signals of nearly equal intensity in the range of 184.3 to 182.9 ppm. This is indicative of an apical/basal form, in which the two phosphorus atoms are nonequivalent. This observation is consistent with density functional theory calculations, which indicate that the most stable structure for $[Fe_2(S_2C_2H_4)(CO)_4(PH_3)_2]$ is the apical/basal isomer, even though the difference in energy between each isomer is weak.[46]

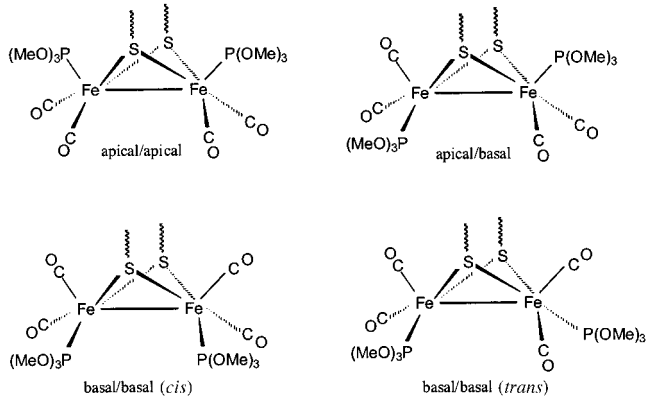


Scheme 2.

The structure of **2** in the solid state was determined by X-ray diffraction and confirms the presence of one phosphite ligand bonded to an iron atom in an apical position (Figure 2). Such an apical orientation for the incoming ligand was previously reported in $[Fe_2(S_2C_3H_6)(CO)_5L]$ when L = $PPh_3$, $PMe_2Ph$, $POEt_3$,[40] NHC,[21,32,33] and $PPh_2\{C_6H_4$-$CCSi(CH_3)_3\}$,[47] whereas the basal position was occupied when L = $P(NC_4H_8)_3$,[48] PTA (1,3,5-triaza-7-phosphaadamantane),[31] $\eta^1$-$Ph_2P$-$CH_2$-$PPh_2$,[23] and $H_2NPr$.[49] Each iron atom in **2** displays the usual pentacoordinate square-pyramidal structure, where both metal centers are displaced from the basal plane toward the apical position by 0.37 Å for Fe(1) and by 0.41 Å for Fe(2).

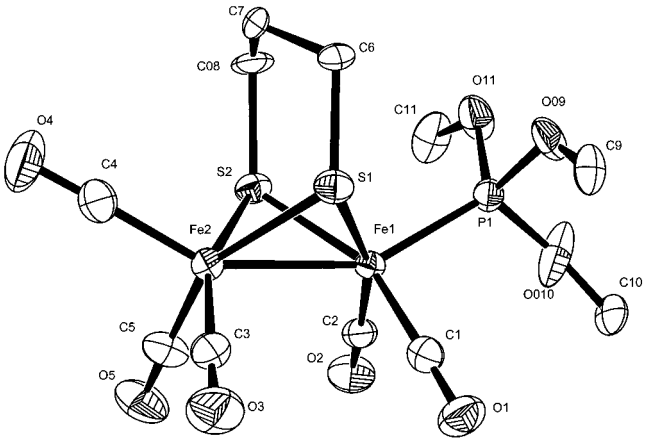


Figure 2. ORTEP diagram of compound **2** depicted with 50% thermal ellipsoids. Selected bond lengths [Å] and angles [°]: Fe(1)–Fe(2) 2.5098(12), Fe(1)–C(1) 1.777(2), Fe(1)–C(2) 1.785(2), C(1)–O(1) 1.144(3), C(2)–O(2) 1.140(3), C(3)–O(3) 1.139(3), Fe(1)–P(1) 2.1618(6), Fe(1)–S(1) 2.2595(6), C(2)–Fe(1)–P(1) 96.89(7), C(1)–Fe(1)–P(1) 97.80(7), P(1)–Fe(1)–S(1) 101.64(2), P(1)–Fe(1)–Fe(2) 150.73(4).

Crystallization of **3** afforded crystals suitable for X-ray diffraction and resulted in the formation of only one isomer in which both phosphite ligands are coordinated in an apical position (Figure 3). It is worth noting that the electrochemically synthesized complex **3** is a *symmetrically* disubstituted diiron compound, as are those prepared by the thermally-activated CO-displacement reaction. Ligand coordination in an apical/apical fashion was previously reported in complexes of type $[Fe_2(S_2C_3H_6)(CO)_4L_2]$, where L = *t*BuNC,[39] $PMe_2Ph$,[40] and $PPh_2(C_6H_4Br)$.[47] In analo-

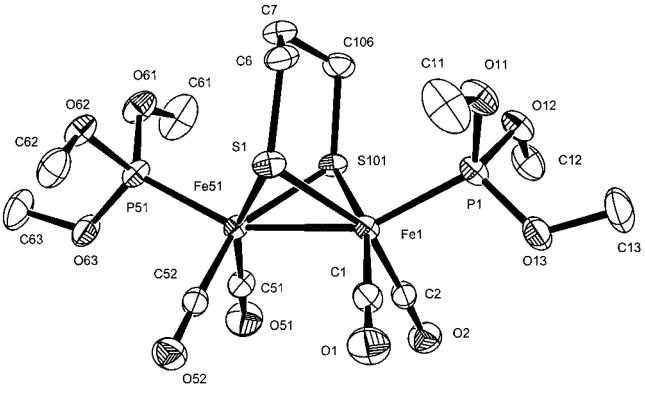


Figure 3. ORTEP diagram of compound **3** depicted with 50% thermal ellipsoids. Selected bond lengths [Å] and angles [°]: Fe(1)–Fe(51) 2.5089(4), Fe(1)–C(1) 1.7763(16), Fe(1)–C(2) 1.7633(16), C(1)–O(1) 1.1443(19), C(2)–O(2) 1.1490(19), Fe(1)–P(1) 2.1656(5), Fe(1)–S(1) 2.268(8), C(2)–Fe(1)–P(1) 97.97(5), C(1)–Fe(1)–P(1) 95.66(5), P(1)–Fe(1)–S(1) 106.8(3), P(1)–Fe(1)–Fe(51) 152.694(13).

  

gous disubstituted complexes, basal/basal *trans* isomers have also been observed in the solid state when L = $PMe_3$[50] and L = PTA,[31] while L = $CN^-$[14] and L = NHC[32] led to basal/apical isomers. These results show that the ligand size is not the determining factor that affects the structure of $[Fe_2(S_2C_3H_6)(CO)_4L_2]$ complexes in the solid state.[36]

The electrochemical properties of organometallic models are one of the interesting features that may lead to a better understanding of the structure–function relationships in the hydrogenase active site. Cyclic voltammetry of **2** and **3** was carried out in $CH_3CN/Bu_4NPF_6$ solution. The monosubstituted complex **2** exhibits two reductions at –1.98 V and –2.29 V and one oxidation at +0.37 V. The primary reduction and oxidation processes of **2** are chemically irreversible. The disubstituted complex **3** exhibits a chemically irreversible reduction at –2.30 V and a chemically reversible oxidation event at 0.12 V. In comparison to **1**, the first reduction processes of compounds **2** and **3** are negatively shifted by 0.31 V and 0.63 V, respectively, which is consistent with the increase in the electron density when one or two CO ligands are replaced by more electron-donating phosphite ligands (see IR data). Another interesting feature of these systems is that the oxidation of phosphite-disubstituted derivatives such as complex **3** and $[Fe_2(S_2C_3H_6)(CO)_4\{P(OEt)_3\}_2]$[40] is a chemically reversible process, while the oxidation of isocyanide- and phosphane-disubstituted derivatives is an irreversible process.[37,39] There is so far no clear agreement on the number of electrons involved in the reduction step of $[Fe_2(S_2C_3H_6)(CO)_{6-x}L_x]$ complexes. For example, Heinekey and co-workers[39] reported that the reduction of $[Fe_2(S_2C_3H_6)(CO)_4(t\text{BuNC})_2]$ is apparently a two-electron process, whereas Sun and co-workers[40] ascribed the first reduction peak of $[Fe_2(S_2C_3H_6)(CO)_{6-x}L_x]$ [L = $PPh_3$, $PMe_2Ph$, $P(OEt)_3$; $x$ = 1,2] to a one-electron process. To determine the number of electrons involved in the reduction and oxidation of **2** and **3**, respectively, we used $[Fe_2(S_2C_3H_6)(CO)_4(I_{Me}CH_2I_{Me})]$ ($I_{Me}$ = 1-methylimidazol-2-ylidene) as an internal standard (see Supporting Information). The chelated dicarbene derivative exhibits a diffusion-limited, reversible, one-electron oxidation process,[26] and its diffusion coefficient should be close to that of **2** and **3**. The voltammetric peak current ($I_p$) for the oxidation of **3** varies linearly with the square root of the potential scan rate ($v$) in the range of 0.02 to 2 $V s^{-1}$. Additionally, the slope of the $I_p$ vs. $v^{1/2}$ plot is more than twice that calculated for the chelated carbene-disubstituted derivative at the same concentration. This clearly demonstrates that the oxidation of **3** is a diffusion-limited, two-electron process. The same procedure allowed us to conclude that the reduction processes of **2** and **3** involve in each case two electrons.

## Protonation Study of Complexes 2 and 3

Before evaluating the electrocatalytic properties of **2** and **3** for proton reduction, it is important to check their reactivity toward protons. The all-CO compound **1** is not reactive toward strong acids such as $HBF_4{\cdot}Et_2O$. However, it is well known that in $[Fe_2(SR)_2(CO)_{6-x}L_x]$ ($x$ = 1,2), the donor ability of the ligand L has a great influence on the nucleophilicity of the $Fe^I$–$Fe^I$ bond.[34] The IR spectrum of a $CH_3CN$ solution of **2** with excess $HBF_4{\cdot}Et_2O$ remains unaltered, which indicates that the replacement of one CO ligand with one $P(OMe)_3$ ligand does not noticeably increase the basicity of the metal–metal bond. Treatment of a $CH_3CN$ solution of **3** with 10 molar equiv. $HBF_4{\cdot}Et_2O$ led to an IR spectrum that displays new $\tilde{\nu}_{CO}$ bands at 2070, 2050, and 2010 $cm^{-1}$. The positive shift of about 80 $cm^{-1}$ is characteristic of the formation of a $Fe^{II}(\mu\text{-H})Fe^{II}$ species.[34] Protonation is, however, very slow since $\nu_{CO}$ bands corresponding to the starting compound **3** were still observed one hour after excess acid was added. The $^1H$ NMR spectrum of **2** recorded at room temperature in the presence of excess $HBF_4{\cdot}Et_2O$ shows a triplet at $\delta$ = –14.8 ppm ($J_{PH}$ = 26.6 Hz) in the high field region, which confirms the formation of a bridging hydride complex.

The electrocatalytic activity of complexes **2** and **3** for proton reduction was investigated in $CH_3CN/Bu_4NPF_6$ solutions with increasing concentrations of toluenesulfonic acid (HOTs, p$K_a$ ca. 8). The addition of HOTs to a solution of **2** triggers the appearance of a new reduction process, noted as B in the cyclic voltammograms in Figure 4. This process occurs at a potential less negative than that of the

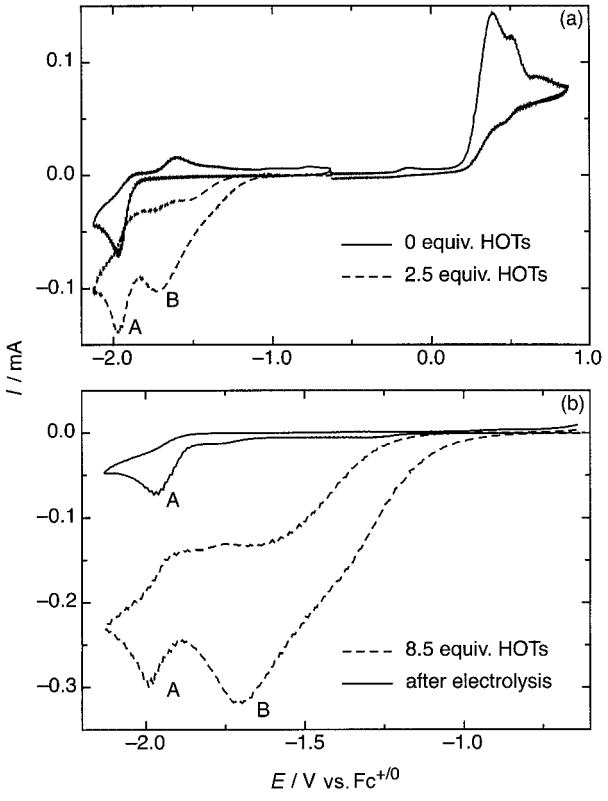


Figure 4. Cyclic voltammograms of compound **2** in $CH_3CN/Bu_4NPF_6$ (a) before and after addition of 2.5 molar equiv. HOTs and (b) after addition of 8.5 molar equiv. HOTs and after electrolysis at –1.65 V. Experimental conditions: $v$ = 0.1 $V s^{-1}$; [**2**] = 2.1 mM; glassy carbon electrode 0.071 $cm^2$ in surface area.

  

reduction of **2**, noted as A in the same Figure. The onset of wave B is at about –1.1 V, and a maximum in height is reached at about –1.7 V. The height of wave B is responsive to the acid concentration. It increases by a factor of three upon increasing the [HOTs]/[**2**] ratio from 2.5 to 8.5 (Figure 4b). Since **2** does not readily react with protons under the present conditions (see IR data above), it is most probable that wave B is due to the reduction of $\mathbf{2}H^+$ generated at the electrode according to the CE mechanism shown in Equations (1), (2), and (3).

$$\mathbf{2} + H^+ \rightleftarrows \mathbf{2}H^+ \quad (1)$$

$$\mathbf{2}H^+ + e^- \rightleftarrows \mathbf{2}H \quad (2)$$

$$2 \times \mathbf{2}H \rightarrow 2 \times \mathbf{2} + H_2 \quad (3)$$

$\mathbf{2}H^+$ does not exist in an appreciable amount in the bulk of the solution, but its reduction at the electrode displaces the protonation equilibrium to the right [Equation (1)]. The amount of acid in solution has a similar effect on this equilibrium, which explains the dependence of the height of wave B on the proton concentration. It is relevant to note that the height of peak A, which corresponds to the reduction of **2**, remains unaffected upon addition of acid. This suggests not only that all the protons available in the diffusion layer are consumed in wave B, but also that the reduction of $\mathbf{2}H^+$ regenerates the unprotonated complex **2**, likely by the release of $H_2$ [Equations (3)]. To support the proposed mechanism, we carried out an electrolysis at –1.65 V of a solution of **2** with 8.5 molar equiv. of HOTs. The charge passed after a period of 120 min was 8.2 F per mol of **2**, consistent with the stoichiometry of one electron and one proton per mol of **2** as proposed in Equations (1)–(3). Gas evolution was observed over the course of the electrolysis, which is consistent with the production of molecular hydrogen, and this has previously been reported for the electrochemical reduction of diiron complexes in the presence of acid.[17,27,29] Cyclic voltammograms recorded after the electrolysis confirms the consumption of almost all of the protons without any noticeable decomposition of **2** (Figure 4b). Despite the presence of excess acid, the hydrogen production seems to proceed through a bimolecular reaction as in Equation (3) and not through the subsequent protonation and reduction of **2**H (i.e. $\mathbf{2}H + H^+ + e^- \rightarrow \mathbf{2} + H_2$). This is most certainly because of the weakly basic character of **2**H, which is either too slowly protonated by HOTs or not protonated at all.

As in the case of compound **2**, the addition of HOTs to a solution of **3** triggers the appearance of a new reduction process, noted as D in the cyclic voltammograms in Figure 5. This process occurs at a potential less negative than that of the reduction of **3**, noted as C in the same Figure. The height of wave D is responsive to the concentration of acid, which indicates proton reduction catalysis (Figure 5b). The onset of this catalysis by **3** occurs at a potential approximately 0.4 V more negative than that for **2**, which parallels the shift in reduction potential. Although **3** seems to be a less efficient catalyst than **2** on the voltammetric timescale, bulk electrolysis at –1.90 V of a solution of **3** containing 8.3 molar equiv. HOTs consumed 8.0 F per mol of **3** over a period of about 120 min. The voltammograms in Figure 5b show that most of the protons were consumed by electrolysis, which suggests that, as in the case of **2**, the catalysis by **3** involves a bimolecular reaction [see Equation (3)].

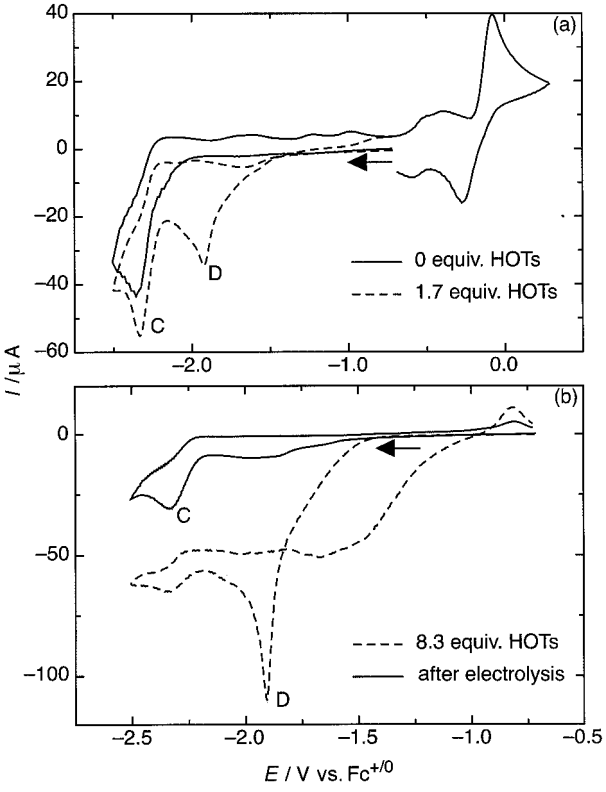


Figure 5. Cyclic voltammograms of compound **3** in $CH_3CN/Bu_4NPF_6$ (a) before and after addition of 1.7 molar equiv. HOTs and (b) after addition of 8.3 molar equiv. HOTs and after electrolysis at –1.9 V. Experimental conditions: $v$ = 0.1 V s$^{-1}$; [**3**] = 2.1 mM; glassy carbon electrode 0.071 cm$^2$ in surface area.

## Conclusions

To summarize our results, we have shown that the electrochemical route represents a convenient method for the selective synthesis of mono- and disubstituted derivatives of diiron dithiolates. We are currently extending this approach to introduce more elaborate ligands (e.g. bidentate ligands) into the coordination sphere of diiron complexes.

Substitution of one CO ligand by one $P(OMe)_3$ ligand shifts the reduction potential of the complex by about 0.3 V. This modification has little effect on the thermodynamics of proton binding. Nevertheless, the voltammogram of **2** in the presence of acid exhibits a reduction wave that does not have a counterpart in the voltammogram of **1**. This is ascribed to proton binding by **2** in the vicinity of the electrode, which is triggered by the more facile reduction of $\mathbf{2}H^+$ relative to that of **2** (CE mechanism). We are presently not able to determine whether the protonation is metal- or ligand- (e.g. sulfur) centered. Bulk electrolysis experiments

  

confirm the occurrence of a CE process and indicate that the proton reduction catalysis occurs most likely by a bimolecular reaction even in the presence of a large excess of acid. It is relevant to note that **2** appears to be a more efficient catalyst in terms of turnovers than the corresponding benzenedithiolate-bridged derivative, whereas the latter works at a significantly less negative potential.[43] This suggests that a careful tailoring of both the bridging and terminal ligands may well lead to an efficient proton reduction catalyst working at a mildly negative potential.

## Experimental Section

**General Procedures:** All reactions were performed under an atmosphere of argon or nitrogen by using conventional Schlenk techniques. Solvents were deoxygenated and dried by standard methods. Literature methods were used for the preparation of $[Fe_2(S_2C_3H_6)(CO)_6]$.[37] All other reagents were commercially available. Bulk electrolysis and cyclic voltammetry experiments were carried out as described elsewhere.[51] Chemical analyses were performed by the Service Central d'Analyse du CNRS (France). IR spectra were recorded in $CH_3CN$ solution with a Nicolet Nexus Fourier transform spectrometer. NMR spectra were recorded with Bruker AMX 3–400 and DRX 500 spectrometers. Single-crystal X-ray diffraction data were collected at 170 K on an X-CALIBUR-2 CCD diffractometer (Oxford Diffraction) with graphite-monochromated Mo-$K_\alpha$ radiation ($\lambda$ = 0.71073 Å). The structures of **2** and **3** were solved by direct methods and refined by full-matrix least-squares on $F^2$.[52] Complete crystal data and parameters for data collection and refinement are listed in Table 1. CCDC-49699 and CCDC-649700 contain the supplementary crystallographic data for this paper. These data can be obtained free of charge from The Cambridge Crystallographic Data Centre via www.ccdc.cam.ac.uk/data_request/cif.

Table 1. Crystallographic data and processing parameters for complexes **2** and **3**.

| Complex | **2** | **3** |
|---|---|---|
| Empirical formula | $C_{11}H_{15}Fe_2O_8PS_2$ | $C_{13}H_{24}Fe_2O_{10}P_2S_2$ |
| Formula weight | 482.02 | 578.08 |
| Crystal system | monoclinic | monoclinic |
| Space group | $P2_1/n$ | $C2/c$ |
| $a$ [Å] | 9.5915(3) | 19.3412(9) |
| $b$ [Å] | 8.8963(2) | 7.8440(3) |
| $c$ [Å] | 21.4503(7) | 15.1964(6) |
| $\beta$ [°] | 96.218(3) | 97.709 |
| $V$ [Å$^3$] | 1819.56(9) | 2284.65(16) |
| $Z$ | 4 | 4 |
| $\rho_{calcd.}$ [g cm$^{-3}$] | 1.756 | 1.681 |
| $\mu$ [mm$^{-1}$] | 1.945 | 1.638 |
| Crystal size [mm] | 0.50 × 0.20 × 0.05 | 0.24 × 0.17 × 0.14 |
| Range of $\theta$ [°] | 2.98–28.88 | 3.66–33.22 |
| Reflections collected | 11908 | 22481 |
| $R_{int}$ | 0.0156 | 0.0332 |
| Unique data/Parameters | 3979/245 | 4121/175 |
| $R(F)$, $wR(F^2)$ (all data) | 0.0354,0.0683 | 0.0475,0.0837 |
| Goodness-of-fit on $F^2$ | 1.063 | 1.047 |
| $\|\Delta\rho\|$ maximum [e Å$^3$] | 0.505 | 0.834 |

**Electrochemical Synthesis of $[Fe_2(S_2C_3H_6)(CO)_5\{P(OMe)_3\}]$ (2):** In a typical procedure, $[Fe_2(S_2C_3H_6)(CO)_6]$ (70 mg, 0.181 mmol) was dissolved in a $N_2$-purged $CH_3CN/Bu_4NPF_6$ solution (15 mL). $P(OMe)_3$ (24 μL, 1.1 molar equiv.) was added by using a microsyringe. Bulk electrolysis was carried out at –1.75 V under vigorous agitation. The color of the solution changed rapidly from orange to brown. After 45–60 min, the quantity of electricity passed reached a plateau value, and the IR spectrum confirmed the total consumption of the starting hexacarbonyl compound. After evaporation of $CH_3CN$ under vacuum, complex **2** was purified by column chromatography on silica gel with hexane/$CH_2Cl_2$ (8:2) as eluent. Yield: 74 mg (85%). IR ($CH_3CN$): $\tilde{\nu}_{CO}$ = 2048 (s), 1991 (vs), 1976 (s), 1938 (w) cm$^{-1}$. $^1$H NMR ($CD_2Cl_2$, 298 K): $\delta$ = 3.75 [d, $^3J_{PH}$ = 11.3 Hz, 9 H, P(O*Me*)$_3$], 2.05 {s br., 4 H, [S-(C*H*$_2$)$_3$-S]}, 1.75 {s br., 1 H, [S-(C*H*$_2$)$_3$-S]}, 1.54 {s br., 1 H, [S-(C*H*$_2$)$_3$-S]} ppm. $^{13}$C{$^1$H} NMR ($CDCl_3$, 298 K): $\delta$ = 211.90 (d, $^2J_{PC}$ = 20.5 Hz, {Fe(*C*O)$_2$[P(OMe)$_3$]}), 209.59 [Fe(*C*O)$_3$], 52.09 [P(O*Me*)$_3$], 30.26, 22.88 [S-(*C*H$_2$)$_3$-S] ppm. $^{31}$P{$^1$H} NMR ($CD_2Cl_2$, 298 K): $\delta$ = 177.04 [*P*(OMe)$_3$] ppm. $^{31}$P{$^1$H} NMR ($CD_2Cl_2$, 183 K): $\delta$ = 186.4 (17%), 184.4 (50%), 178.0 (25%), 177.1 (8%), [*P*(OMe)$_3$] ppm. LSMIS: *m*/*z* calcd. for [M]$^+$ 481.9; found 481.9. $C_{11}H_{15}Fe_2O_8PS_2$ (482.02): calcd. C 27.41, H 3.14; found C 27.90, H 3.40.

**Electrochemical Synthesis of $[Fe_2(S_2C_3H_6)(CO)_4\{P(OMe)_3\}_2]$ (3):** Complex **3** was prepared as described for complex **2** except that the amount of added $P(OMe)_3$ was 2.1 equiv. and that the electrolysis potential was set to –2.0 V. Yield (starting from 70 mg **1**): 71 mg (68%). IR ($CH_3CN$): $\tilde{\nu}_{CO}$ = 2004 (s), 1966 (vs), 1937 (s), 1917 (w) cm$^{-1}$. $^1$H NMR ($CDCl_3$, 298 K): $\delta$ = 3.77 [d, $^3J_{PH}$ = 11.7 Hz, 18 H, 2 P(O*Me*)$_3$], 1.94 {m br., 4 H, [S-(C*H*$_2$)$_3$-S]}, 1.70 {s br., 2 H, [S-(C*H*$_2$)$_3$-S]} ppm. $^{13}$C{$^1$H} NMR ($CDCl_3$, 298 K): $\delta$ = 213.50 (d, $^2J_{PC}$ = 17 Hz, {Fe(*C*O)$_2$[P(OMe)$_3$]}), 51.67 [P(O*Me*)$_3$], 29.94, 22.03 [S-(*C*H$_2$)$_3$-S] ppm. $^{31}$P{$^1$H} NMR ($CD_2Cl_2$, 298 K): $\delta$ = 180.40 [*P*(OMe)$_3$] ppm. LSMIS: *m*/*z* calcd. for [M]$^+$ 577.9; found 577.9. $C_{13}H_{24}Fe_2O_{10}P_2S_2$ (578.08): calcd. C 27.01, H 4.18, P 10.72; found C 27.04, H 4.16, P 10.32.

**Supporting Information** (see footnote on the first page of this article): Plots as a function of the potential scan rate of the oxidation current of compound **3** and $[Fe_2(S_2C_3H_6)(CO)_4(I_{Me}CH_2I_{Me})]$ ($I_{Me}$ = 1-methylimidazol-2-ylidene) used as an internal standard, cyclic voltammetry of **1** and **2** in the presence of added $P(OMe)_3$, along with the kinetic analysis of the charge-transfer-catalyzed substitution process, are presented.

## Acknowledgments

We are grateful to the Centre National de Recherche Scientifique (CNRS), the Agence National de la Recherche (ANR, project number: NT05-2_42699 – PhotoBioH2), and the University of Brest for financial support of this work.

[1] M. Frey, *ChemBioChem* **2002**, *3*, 153–160.
[2] Y. Nicolet, B. J. Lemon, J. C. Fontecilla-Camps, J. W. Peters, *Trends Biochem. Sci.* **2000**, *25*, 138–143.
[3] M. Y. Darensbourg, E. J. Lyon, J. J. Smee, *Coord. Chem. Rev.* **2000**, *206–207*, 533–561.
[4] R. B. King, T. E. Bitterwolf, *Coord. Chem. Rev.* **2000**, *206–207*, 563–579.
[5] M. Y. Darensbourg, E. J. Lyon, X. Zhao, I. P. Georgakaki, *Proc. Natl. Acad. Sci. USA* **2003**, *100*, 3683–3688.
[6] D. J. Evans, C. J. Pickett, *Chem. Soc. Rev.* **2003**, *32*, 268–275.
[7] T. B. Rauchfuss, *Inorg. Chem.* **2004**, *43*, 14–26.
[8] V. Artero, M. Fontecave, *Coord. Chem. Rev.* **2005**, *249*, 1518–1535.
[9] S. P. Best, *Coord. Chem. Rev.* **2005**, *249*, 1536–1554.
[10] J.-F. Capon, F. Gloaguen, P. Schollhammer, J. Talarmin, *Coord. Chem. Rev.* **2005**, *249*, 1664–1676.

  

[11] L. Sun, B. Akermark, S. Ott, *Coord. Chem. Rev.* **2005**, *249*, 1653–1663.
[12] A. Le Cloirec, S. P. Best, S. Borg, S. C. Davies, D. J. Evans, D. L. Hughes, C. J. Pickett, *Chem. Commun.* **1999**, 2285–2286.
[13] E. J. Lyon, I. P. Georgakaki, J. H. Reibenspies, M. Y. Darensbourg, *Angew. Chem. Int. Ed.* **1999**, *38*, 3178–3180.
[14] M. Schmidt, S. M. Contakes, T. B. Rauchfuss, *J. Am. Chem. Soc.* **1999**, *121*, 9736–9737.
[15] J. D. Lawrence, H. Li, T. B. Rauchfuss, M. Benard, M. M. Rohmer, *Angew. Chem. Int. Ed.* **2001**, *40*, 1768–1771.
[16] P. Das, J. F. Capon, F. Gloaguen, F. Y. Petillon, P. Schollhammer, J. Talarmin, K. W. Muir, *Inorg. Chem.* **2004**, *43*, 8203–8205.
[17] S. Ott, M. Kritikos, B. Akermark, L. C. Sun, R. Lomoth, *Angew. Chem. Int. Ed.* **2004**, *43*, 1006–1009.
[18] J. L. Stanley, T. B. Rauchfuss, S. R. Wilson, *Organometallics* **2007**, *26*, 1907–1911.
[19] C. Tard, X. M. Liu, S. K. Ibrahim, M. Bruschi, L. De Gioia, S. C. Davies, X. Yang, L. S. Wang, G. Sawers, C. J. Pickett, *Nature* **2005**, *433*, 610–613.
[20] G. Zampella, M. Bruschi, P. Fantucci, M. Razavet, C. J. Pickett, L. De Gioia, *Chem. Eur. J.* **2005**, *11*, 509–520.
[21] L. L. Duan, M. Wang, P. Li, Y. Na, N. Wang, L. C. Sun, *Dalton Trans.* **2007**, 1277–1283.
[22] S. Ezzaher, J. F. Capon, F. Gloaguen, F. Y. Petillon, P. Schollhammer, J. Talarmin, R. Pichon, N. Kervarec, *Inorg. Chem.* **2007**, *46*, 3426–3428.
[23] W. M. Gao, J. Ekstrom, J. H. Liu, C. N. Chen, L. Eriksson, L. H. Weng, B. Akermark, L. H. Sun, *Inorg. Chem.* **2007**, *46*, 1981–1991.
[24] G. Hogarth, I. Richards, *Inorg. Chem. Commun.* **2007**, *10*, 66–70.
[25] A. K. Justice, G. Zampella, L. DeGioia, T. B. Rauchfuss, J. I. vanderVlugt, S. R. Wilson, *Inorg. Chem.* **2007**, *46*, 1655–1664.
[26] D. Morvan, J. F. Capon, F. Gloaguen, A. LeGoff, M. Marchivie, F. Michaud, P. Schollhammer, J. Talarmin, J. J. Yaouanc, R. Pichon, N. Kervarec, *Organometallics* **2007**, *26*, 2042–2052.
[27] D. S. Chong, I. P. Georgakaki, R. Mejia-Rodriguez, J. Samabria-Chinchilla, M. P. Soriaga, M. Y. Darensbourg, *Dalton Trans.* **2003**, 4158–4163.
[28] S. J. Borg, T. Behrsing, S. P. Best, M. Razavet, X. M. Liu, C. J. Pickett, *J. Am. Chem. Soc.* **2004**, *126*, 16988–16999.
[29] F. Gloaguen, J. D. Lawrence, T. B. Rauchfuss, *J. Am. Chem. Soc.* **2001**, *123*, 9476–9477.
[30] F. Gloaguen, J. D. Lawrence, T. B. Rauchfuss, M. Benard, M. M. Rohmer, *Inorg. Chem.* **2002**, *41*, 6573–6582.
[31] R. Mejia-Rodriguez, D. S. Chong, J. H. Reibenspies, M. P. Soriaga, M. Y. Darensbourg, *J. Am. Chem. Soc.* **2004**, *126*, 12004–12014.
[32] J. F. Capon, S. ElHassnaoui, F. Gloaguen, P. Schollhammer, J. Talarmin, *Organometallics* **2005**, *24*, 2020–2022.
[33] J. W. Tye, J. Lee, H. W. Wang, R. Mejia-Rodriguez, J. H. Reibenspies, M. B. Hall, M. Y. Darensbourg, *Inorg. Chem.* **2005**, *44*, 5550–5552.
[34] K. Fauvel, R. Mathieu, R. Poilblanc, *Inorg. Chem.* **1976**, *15*, 976–978.
[35] M. Bruschi, P. Fantucci, L. De Gioia, *Inorg. Chem.* **2003**, *42*, 4773–4781.
[36] J. A. De Beer, R. J. Haines, *J. Organomet. Chem.* **1972**, *37*, 173–181.
[37] F. Gloaguen, J. D. Lawrence, M. Schmidt, S. R. Wilson, T. B. Rauchfuss, *J. Am. Chem. Soc.* **2001**, *123*, 12518–12527.
[38] J. D. Lawrence, T. B. Rauchfuss, S. R. Wilson, *Inorg. Chem.* **2002**, *41*, 6193–6195.
[39] J. L. Nehring, D. M. Heinekey, *Inorg. Chem.* **2003**, *42*, 4288–4292.
[40] P. Li, M. Wang, C. J. He, G. H. Li, X. Y. Liu, C. N. Chen, B. Akermark, L. C. Sun, *Eur. J. Inorg. Chem.* **2005**, 2506–2513.
[41] A. Darchen, H. Mousser, H. Patin, *J. Chem. Soc. Chem. Commun.* **1988**, 968–970.
[42] J. I. van der Vlugt, T. B. Rauchfuss, S. R. Wilson, *Chem. Eur. J.* **2005**, *12*, 90–98.
[43] F. Gloaguen, D. Morvan, J.-F. Capon, P. Schollhammer, J. Talarmin, *J. Electroanal. Chem.* **2007**, *603*, 15–20.
[44] E. J. Lyon, I. P. Georgakaki, J. H. Reibenspies, M. Y. Darensbourg, *J. Am. Chem. Soc.* **2001**, *123*, 3268–3278.
[45] X. Zhao, I. P. Georgakaki, M. L. Miller, R. Mejia-Rodriguez, C. Y. Chiang, M. Y. Darensbourg, *Inorg. Chem.* **2002**, *41*, 3917–3928.
[46] J. W. Tye, M. Y. Darensbourg, M. B. Hall, *Inorg. Chem.* **2006**, *45*, 1552–1559.
[47] J. Ekstrom, M. Abrahamsson, C. Olson, J. Bergquist, F. B. Kaynak, L. Eriksson, S. C. Licheng, H. C. Becker, B. Akermark, L. Hammarstrom, S. Ott, *Dalton Trans.* **2006**, 4599–4606.
[48] J. Hou, X. J. Peng, Z. Y. Zhou, S. G. Sun, X. Zhao, S. Gao, *J. Organomet. Chem.* **2006**, *691*, 4633–4640.
[49] L. Schwartz, J. Ekstrom, R. Lomoth, S. Ott, *Chem. Commun.* **2006**, 4206–4208.
[50] X. Zhao, I. P. Georgakaki, M. L. Miller, J. C. Yarbrough, M. Y. Darensbourg, *J. Am. Chem. Soc.* **2001**, *123*, 9710–9711.
[51] J.-F. Capon, F. Gloaguen, P. Schollhammer, J. Talarmin, *J. Electroanal. Chem.* **2004**, *566*, 241–247.
[52] Programs used: a) G. M. Sheldrick, *SHELX97*, University of Göttingen, Germany, **1998**; b) *WinGX – A Windows Program for Crystal Structure Analysis*: L. J. Farrugia, *J. Appl. Crystallogr.* **1999**, *32*, 837–838.

Received: June 8, 2007
Published Online: September 24, 2007

  